BIOCHEMISTRY
including biophysical chemistry & molecular biology

Article

pubs.acs.org/biochemistry

Phosphorylation of the Kinase Domain Regulates Autophosphorylation of Myosin IIIA and Its Translocation in Microvilli

Byung Chull An,[†] Tsuyoshi Sakai,[†,‡] Shigeru Komaba,[†] Hiroko Kishi,[§] Sei Kobayashi,[§] Jin Young Kim,[∥] Reiko Ikebe,[†,‡] and Mistuo Ikebe*[,†,‡]

[†]Department of Microbiology and Physiological Systems, University of Massachusetts Medical School, Worcester, Massachusetts 01605, United States

[‡]Department of Cellular and Molecular Biology, University of Texas Health Science Center at Tyler, Tyler, Texas75708, United States

[§]Department of Molecular Physiology and Medical Bioregulation, Yamaguchi University Graduate School of Medicine, Ube 755-8505, Japan

[∥]Division of Mass Spectrometry, Korea Basic Science Institute, Ochang-eup, Cheongwon-gun, Chungbuk 363-883, Korea

Supporting Information

ABSTRACT: Motor activity of myosin III is regulated by autophosphorylation. To investigate the role of the kinase activity on the transporter function of myosin IIIA (Myo3A), we identified the phosphorylation sites of kinase domain (KD), which is responsible for the regulation of kinase activity and thus motor function. Using mass spectrometry, we identified six phosphorylation sites in the KD, which are highly conserved among class III myosins and Ste20-related misshapen (Msn) kinases. Two predominant sites, Thr[184] and Thr[188], in KD are important for phosphorylation of the KD as well as the motor domain, which regulates the affinity for actin. In the Caco2 cells, the full-length human Myo3A (hMyo3AFull) markedly enlarged the microvilli, although it did not show discrete localization within the microvilli. On the other hand, hMyo3AFull(T184A) and hMyo3AFull(T188A) both showed clear localization at the microvilli tips. Our results suggest that Myo3A induces large actin bundle formation to form microvilli, and phosphorylation of KD at Thr[184] and Thr[188] is critical for the kinase activity of Myo3A, and regulation of Myo3A translocation to the tip of microvilli. Retinal extracts potently dephosphorylate both KD and motor domain without IQ motifs (MDIQo), which was inhibited by okadaic acid (OA) with nanomolar range and by tautomycetin (TMC) with micromolar range. The results suggest that Myo3A phosphatase is protein phosphatase type 2A (PP2A). Supporting this result, recombinant PP2Ac potently dephosphorylates both KD and MDIQo. We propose that the phosphorylation−dephosphorylation mechanism plays an essential role in mediating the transport and actin bundle formation and stability functions of hMyo3A.

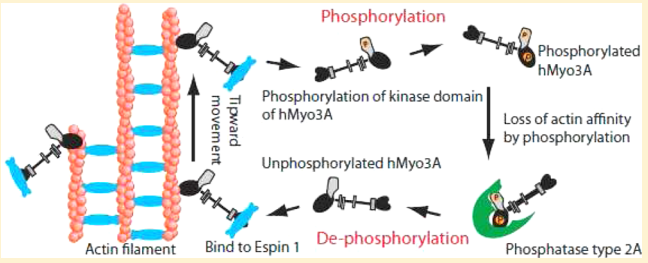

Class III myosin, a member of the myosin superfamily, is unique in having an N-terminal kinase domain joined to a myosin motor domain.[1] Myosin III is found in the photoreceptor cell of the eye and the stereocilia of the inner ear hair cells.[2,3] In vertebrates, two isoforms of class III myosin, myosin IIIA (Myo3A) and myosin IIIB (Myo3B), have been found,[4,5] of which most studies have been done with Myo3A. The human myosin IIIA (hMyo3A) is responsible for progressive non-syndromic hearing loss in humans (DFNB30),[6] and a mouse model shows age-dependent degeneration of the stereocillia in inner ear hair cells.[7] The physiological function of hMyo3A is still unknown, but recent studies have suggested that hMyo3A may function as a cargo carrier.[8−10]

Immunohistochemical studies have shown that Myo3A localizes at the tip of stereocillia in inner ear hair cells.[3] Fish myosin IIIA (bMyo3A) accumulates in the distal ends of rod and cone ellipsoid and colocalizes with the plus-distal ends of inner segment actin filament bundles, where actin forms the microvilli-like calycal processes.[2] Furthermore, GFP−bMyo3A localizes at the tip of filopodia in Hela cells.[11] Since the plus-end of actin filaments of the actin bundles in filopodia localizes at the tips, the localization of bMyo3A at the filopodial tips suggests that this myosin traveled on actin filaments and accumulated at the end of the actin track. Supporting this view, it was found that hMyo3A has an extremely high affinity for actin in its dephosphorylated form,[12,13] while it has very slow actin-translocating velocity, which is consistent with low actin-activated ATPase activ-

Received: October 2, 2014
Revised: November 14, 2014
Published: November 17, 2014

   dx.doi.org/10.1021/bi501247z | *Biochemistry* 2014, 53, 7835−7845

ity.[14,12,15] Recently, it was found that espin 1, which has an activity of actin filament elongation, binds myosin III, which suggested that myosin III plays a role in transporting espin 1.[16] These findings further supported that myosin III may function as a cargo transporter.

A critical issue is that autophosphorylation markedly reduces the affinity for actin,[12,13] suggesting that this is an important regulatory mechanism for the function of myosin III. Since myosin III phopshorylates by itself, it is postulated that regulation of phosphorylation is achieved by protein phosphatases, although the identity of such protein phosphatases is unknown. It is suggested that autophosphorylation of the Myo3A motor may act as a means for its regulation in photoreceptors and inner ear hair cells under specific cellular conditions.[17]

Another important question is the functional significance of myosin IIIA in actin cytoskeletal reorganization. Myosin IIIA is found in stereocilia in sensory hair cells, and a myosin IIIA aberration causes outer hair cell degeneration.[7] Moreover, overexpression of myosin IIIA results in elongation of stereocilia.[16] These results suggest the involvement of myosin IIIA in the structural integrity of the actin cytoskeleton.

In the present study, we identified the phosphorylation sites in the kinase domain (KD), which are important for the kinase activity of Myo3A and thus translocation of myosin in cells. We found that two identified phosphorylation sites are important for the regulation of hMyo3A localization on actin-bundle based structures of microvilli in cells. Moreover, we identified that protein phosphatase type 2A is responsible for dephosphorylation of Myo3A. These findings are a major step toward understanding the regulation mechanism of hMyo3A function in vivo. It should be noted that one of our identified sites (Thr^{184}) was quite recently reported from another group.[18] Interestingly, myosin IIIA enlarges the slender actin bundles produced by espin 1 to thick and long microvilli-like protrusive structures.

EXPERIMENTAL PROCEDURES

Reagents and Protein. Rabbit skeletal muscle actin was purified according to Spudich and Watt,[19] and actin filaments were stabilized by phalloidin. Restriction enzymes and modifying enzymes were purchased from New England Biolabs (Beverly, MA). Formic acid, ammonium bicarbonate, urea, dithiothreitol (DTT), and iodoacetamide (IAA) were purchased from Sigma-Aldrich (St. Louis, MO). Sequencing-grade modified trypsin was purchased from Promega (Madison, WI). HPLC-grade acetonitrile was purchased from Burdick and Jackson (Muskegon, MI). Water was purified using a Milli Q system (Millipore, Molsheim, France). Smooth muscle myosin RLC (LC_{20}) was expressed in *Escherichia coli* and purified as described.[20,21] PP2Ac and PP1c genes were cloned into pFast-Bac1 baculovirus transfer vector (Life technologies, Carlsbad, CA) containing FLAG-tag from rat cDNA. Smooth muscle MLCK was purified from turkey gizzard as described.[22]

Generation of the Human Myosin IIIA Construct. Total RNA was prepared from human retinal pigment epithelia cell line ARPE-19 (ATCC, Manassas, VA) using an RNeasy minikit (Qiagen, Hilden, Germany). Poly(A)$^+$ RNA was isolated using an Oligotex mRNA minikit (Qiagen, Hilden, Germany). Human myosin IIIA (hMyo3A) cDNA was generated by reverse transcription (Superscript reverse transcriptase II; Life technologies, Carlsbad, CA) with specific primers.

The amplified DNA fragments were ligated into pFast-Bac1 baculovirus transfer vector (Life technologies, Carlsbad, CA), containing FLAG-tag or 6xHis-tag at the C-terminus, or GST-tag at the N-terminus. Alanine point mutations were created by site-directed mutagenesis.[23] All of the clones were sequence verified. The recombinant baculovirus expressing hMyo3A derivatives was produced according to the manufacturer's protocol.

Expression and Purification of hMyo3A Variants and PPases. To express recombinant hMyo3A and PPases, 200 mL of sf9 cells (about 1×10^9 cells) was infected with each virus expressing hMyo3A variant. The infected cells were cultured for 3 days at 28 °C. The FLAG-fused recombinant proteins were purified from sf9 cells using 100 μL of anti-FLAG affinity column, and bound proteins were eluted by FLAG peptide in an elution buffer.[24,25] The 6xHis-fused recombinant proteins were purified from sf9 cells using 100 μL of native Ni-NTA column and eluted with a linear gradient of 200 to 500 mM imidazole in PBS buffer.[12] Baculoviruses expressing GST-fused recombinant proteins were lysed in 20 mM HEPES (pH 7.5), 400 mM NaCl, and 5 mM β-mercaptoethanol, and the supernatant was applied to 100 μL of glutathione−Sepharose resin (GE Healthcare, Wauwatosa, WI). Fusion proteins were eluted off the GST beads in an elution buffer containing 50 mM Tris-HCl (pH 8.0), 10 mM glutathione.[26] The purified proteins were stored at −70 °C after buffer change (PBS buffer with 10% glycerol). The protein concentration was measured using the Bradford method, with BSA as the standard.

Gel Electrophoresis Analysis. SDS-PAGE was carried out on a 7.5−20% polyacrylamide gel using the discontinuous buffer system of Laemmli.[27] Molecular mass markers used were smooth muscle myosin heavy chain (204 kDa), galactosidase (116 kDa), phosphorylase *b* (97.4 kDa), bovine serum albumin (66 kDa), ovalbumin (45 kDa), carbonic anhydrase (29 kDa), myosin regulatory light chain (20 kDa), and lactalbumin (14.2 kDa). Gel was stained with Coomassie Brilliant Blue R-250.

LC-MS/MS Analysis and Database Search. LC-MS/MS analysis was performed independently in two laboratories: Yamaguchi University (Japan) and Korea Basic Science Institute (Korea). In Yamaguchi University, the protein sample was separated by SDS-PAGE and transferred to PVDF membrane and stained by CBB to visualize protein. The KD band was excised and subjected to mass spectrometry. Proteins on the PVDF were reduced with DTT at 65 °C for 1 h and carboxymethylated with monoiodoacetic acid. After the PVDF was washed with 2% acetonitrile, the proteins on the PVDF membrane were digested either with Lys-C or trypsin at 37 °C for 18 h. The digested peptides were desalted with ZipTipC18 (Millipore), dried, and redissolved in 2% acetonitrile and 0.1% formic acid. Peptides were separated by one-dimensional liquid chromatography (DiNa, KYA technology, Tokyo, Japan) equipped with reversed phase C18 column. The mobile phases, A and B, consist of 2% acetonitrile, 0.1% formic acid, and 70% acetonitrile, 0.1% formic acid, respectively. The separated peptides were introduced into a quadruple-linear ion trap tandem mass spectrometer (4000QTRAP, AB SCIEX) equipped with Picotip emitter (New Objectives). The MS/MS spectra of phosphopeptides were acquired either by Prec79(−)-triggered IDA (information based data acquisition) or MRM (multiple reaction monitoring)-triggered IDA. The acquired MS/MS spectra were then subjected to database search using either Mascot (Matrix Sciences) or ProteinPilot (AB SCIEX) to determine phosphorylation sites. The phosphorylation sites determined in all sample preparations (both Lys-C and trypsin digestion), all data acquisitions (both Prec79(−)-triggered IDA and MRM-triggered IDA), and all database search (Mascot and

ProteinPilot) were Ser^{73}, Ser^{177}, Ser^{178}, Thr^{184}, Thr^{188}, and Thr^{302}.

In the Korea Basic Science Institute, the experiment was done as follows: Proteins were separated by SDS-PAGE and "in gel digestion" was performed with trypsin (1:50 proteinase-to-protein) as described.[28] In brief, bands were washed and digested by trypsin at 37 °C for 16 h in 50 mM ammonium bicarbonate. The peptide samples were dissolved in mobile phase A for Nano-LC/ESI-MS/MS. Peptides were identified using MS/MS with a nano-LC-MS system consisting of nanoACQUITY Ultra-Performance LC System (Waters Corporation, Milford, MA) and a LTQ FT mass spectrometer (Thermo Scientific, West Palm Beach, FL) equipped with a nanoelectrospray source. An autosampler was used to load the peptide solutions onto a C18 trap-column (Waters Corporation, Milford, MA). The peptides were desalted and concentrated, and then the trapped peptides were separated on a 150 mm homemade microcapillary C18 column.

The mobile phases, A and B, were composed of 0% and 100% acetonitrile, respectively, and each contained 0.1% formic acid. The LC gradients used are 5% B for 5 min, 15% B for 5 min, 50% B for 70 min, 95% B for 5 min. We applied 95% B for the next 5 min and 5% B for another 5 min. The voltage for an electrospray was 2.5 kV. In each duty circle of mass analysis, one high-mass resolution (100 000) MS spectrum was acquired using the FT-ICR analyzer, followed by five data-dependent MS/MS scans using the linear ion trap analyzer. For MS/MS analysis, normalized collision energy (35%) was used throughout the collision-induced dissociation (CID) phase.

All MS/MS spectral data were manually analyzed for peptide identification. Oxidized methionine and carbamidomethylated cysteine (only for reduced and alkylated protein sample) were considered as a modification. MS/MS spectra were analyzed with Proteome Discoverer (version 1.4, Thermo Scientific, West Palm Beach, FL) against the Myosin-IIIa protein database (Uniprot number Q8NEV4). Proteome Discoverer was used with a monoisotopic mass selected, a precursor mass error of 25 ppm, and a fragment ion mass error of 0.8 Da. Full tryptic peptides were selected with two potential miscleavage. Phosphorylations at serine, threonine, and tyrosine residues and oxidation at methionine residues were considered as variable modifications. Carbamidomethylated cysteine was chosen as a fixed modification. Only peptides with high confidence are included. All MS/MS spectra identified as modified peptides were manually confirmed.

Kinase Assay. Autophosphorylation of hMyo3A-KD variants was detected by incorporation of ^{32}P using [γ-^{32}P]ATP. The reaction was done in the buffer containing 30 mM HEPES (pH 7.5), 30 mM KCl, 2 mM $MgCl_2$, 1 mM EGTA, 1 mM DTT, 1 μM microcystin-LR, 250 μM cold ATP, and 250 μCi of [γ-^{32}P]ATP (1000 Ci/mmol) (GE Healthcare, Wauwatosa, WI) at 25 °C. The phosphorylated hMyo3A variants were subjected to SDS-PAGE, and the incorporation of ^{32}P into phosphorylated kinase domain was detected by phosphorimaging using the Typhoon 9410 variable mode imager (GE Healthcare, Wauwatosa, WI). Following phosphorimaging, the gel was stained with Coomassie Brilliant Blue R-250.

Actin Activated ATPase Assay. The ATPase activity was measured in buffer A (30 mM HEPES (pH 7.5), 30 mM KCl, 2 mM $MgCl_2$, 1 mM EGTA, 1 mM DTT, 1 μM microcystin-LR, 1 mM ATP) in the presence of 0.036 μM hMyo3A-MDIQo with or without kinase domain variants in the presence of an ATP regeneration system (20 units/mL pyruvate kinase and 2 mM phosphoenolpyruvate) at 25 °C.[29] hMyo3A-MDIQo was preincubated with hMyo3A-KD variants for 1 h in the absence of actin; then actin-activated ATPase activity was monitored after addition of actin (10 μM final). Data fitting and analysis were performed by using GraphPad Prism.

PPase Assay. The hMyo3A-KD, hMyo3A-MDIQo, and LC_{20} were phosphorylated and used as substrates of PPases. The autophosphorylation of hMyo3A-KDs was done in the buffer containing 30 mM HEPES (pH 7.5), 30 mM KCl, 2 mM $MgCl_2$, 1 mM EGTA, 1 mM DTT, and 50 μM [γ-^{32}P]ATP for 1 h at 25 °C. HMyo3A-MDIQo (36 nM) was phosphorylated by 36 nM hMyo3A-KD(WT) in the buffer containing 30 mM HEPES (pH 7.5), 30 mM KCl, 2 mM $MgCl_2$, 1 mM EGTA, 1 mM DTT, and 50 μM [γ-^{32}P]ATP for 1 h at 25 °C. LC_{20} (5 μM) was phosphorylated by MLCK (5 μg/mL) in the buffer containing 50 μg/mL of calmodulin (CaM), 25 mM MOPS (pH 7.2), 12.5 mM β-glycerol-phosphate, 25 mM $MgC1_2$, 5 mM EGTA, 2 mM EDTA, 0.25 mM DTT, and 50 μM [γ-^{32}P]ATP for 20 min at 25 °C.

The PPase activity was measured in 1 mM $MgCl_2$, 40 mM KCl, 30 mM Tris·HCl (pH 7.5), 5 mM DTT, 0.5−10 nM PPase, and 2 mM cold-ATP with or without PPase inhibitors for 30 min at 25 °C. All assays were initiated by adding PPase to the reaction mixture. The reaction mixture was subjected to SDS-PAGE, and the incorporation of ^{32}P into the protein was measured by phosphorimaging using the Typhoon 9410 variable mode imager (GE Healthcare, Wauwatosa, WI). Following phosphorimaging, the gel was stained with Coomassie Brilliant blue R-250. Data fitting and analysis were performed using GraphPad Prism.

GST-Pull Down Assay. A 30-μL sample of 50% slurry of glutathione−Sepharose 4B beads (GE Healthcare, Wauwatosa, WI) was equilibrated in PBS buffer (2.7 mM KCl, 137 mM NaCl, 10 mM Na_2HPO_4, and KH_2PO_4). GST-hMyo3A-KD(D150N) variants (10 μg) were phosphorylated with 1 μg of KD(WT)-flag for 1 h in total volume of 20 μL. The slurry was mixed with 10 μg of GST-hMyo3A-KD variants and 3 μg of hMyo3A-MDIQo in total volume of 100 μL and then incubated for 1 h at 4 °C on a rotator. The beads were washed three times with 1 mL of the PBS buffer, and then SDS loading buffer was added to the samples, and the mixture was heated at 100 °C for 5 min. Proteins were loaded on 12% SDS-PAGE and stained by Coomassie Brilliant blue R-250.

Cell Culture and Transfection. Caco2 cells (ATCC) were cultured with Dulbecco's modified Eagle's medium (DMEM) containing 10% fetal bovine serum (FBS). The cells were kept in 5% CO_2 at 37 °C. BD-Matrigel (BD biosciences, San Jose, CA; Catalog No. 356237) was used as a substrate for culturing the cells. Transient transfections were performed with Lipofectamine 2000 (Life technologies, Carlsbad, CA) according to the manufacture's instructions. Plasmid DNA was purified using Qiagen mini- or maxi-prep columns. The cells were observed at 20 h after transfection. Actin was stained with Alexa 488-phalloidin.

Cell Fixation. Cells cultured on glass coverslips were fixed with a fixation buffer (4% formaldehyde, 2 mM $MgCl_2$, 1 mM EGTA in PBS) for 20 min at room temperature, washed twice with PBS, and mounted using Prolong Gold antifade reagent (Life technologies, Carlsbad, CA). For actin staining, cells were permeabilized with 0.05% Triton X-100 in PBS for 10 min at room temperature and stained with Alexa Fluor 488 phalloidin (Life technologies, Carlsbad, CA).

Confocal Microscopy. Fluorescence images were obtained with a Leica DM IRB laser scanning confocal microscope

controlled by Leica TCS SP II systems (Leica Microsystems, Wetzlar, Germany) equipped with a Plan-Apochromat 60× 1.40 NA oil immersion objective (Leica Microsystems, Wetzlar, Germany). The images were processed using Photoshop software (Adobe Systems, San Jose, CA).

RESULTS

Identification of Autophosphorylation Sites in KD of Human Myo3A. We expressed N-terminal KD using a baculovirus expression system (Figure 1A). The expressed KD

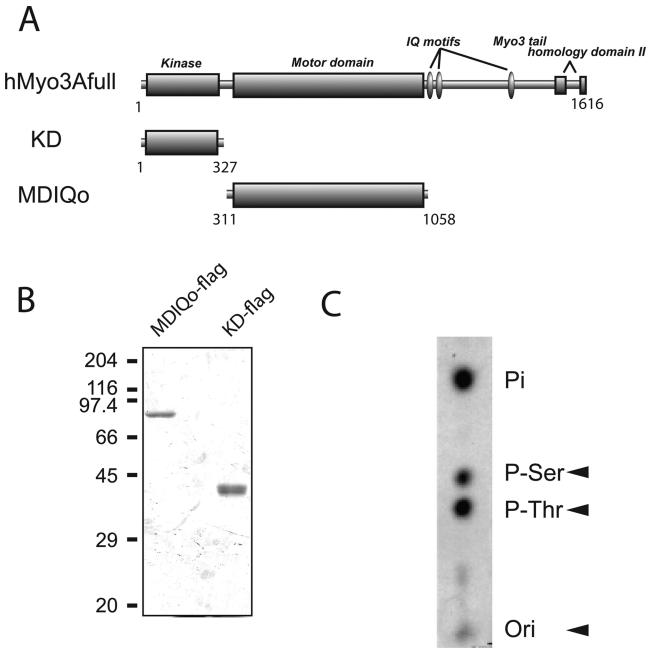

Figure 1. Schematic diagram and purification of hMyo3A constructs. (A) hMyo3A constructs used in this study. Numbers are amino acid numbers of hMyo3A. KD, kinase domain of hMyo3A; MDIQo, motor domain without IQ motifs of hMyo3A. (B) SDS-PAGE of purified hMyo3A constructs. (C) Phosphoamino acid analysis of autophosphorylated KD. The arrowheads indicate migrations of standard phosphoamino acids (P-Ser, P-Thr) and origin of sample application (Ori).

having FLAG-tag was purified using anti-FLAG affinity chromatography, and KD with an apparent molecular mass of 40 kDa was purified (Figure 1B). We first performed a phosphoamino acid analysis of autophosphorylated KD and found that threonine residues are predominantly phosphorylated (Figure 1C). To identify the phosphorylation sites, we performed a mass spectrometry analysis. The KD band in the SDS-PAGE gel was excised, digested in gel, and subjected to a mass spectrometry analysis as described in Experimental Procedures. Mass spectrometry analysis was done for both phosphorylated and unphosphorylated KD. Six phosphorylation sites in KD were identified by MS/MS, Ser^{73}, Ser^{177}, Thr^{178}, Thr^{184}, Thr^{188}, and Thr^{302} (Figure S1A, Supporting Information). The results from the mass spectroscopy analysis for Thr^{184} and Thr^{188} are shown in Figure S1B, Supporting Information. Among the identified six phosphorylation sites, four of the phosphorylated sites were located at the activation loop (Ser^{177}, Thr^{178}, Thr^{184}, and Thr^{188} in hMyo3A-KD).

It is known that the kinase domain of myosin IIIA (Myo3A) shows high homology in different species. Among the identified residues, Ser^{177}, Thr^{178}, Thr^{184}, and Thr^{188}, but not Ser^{73} and Thr^{302}, are conserved among various species (Figure S2A, Supporting Information).

The human Myo3A kinase domain has more than 41% homology with Msn kinases belonging to the STE20 kinase family, and Ser^{177}, Thr^{178}, Thr^{184}, and Thr^{188} are also conserved among Msn kinases (Figure S1A, Supporting Information). Figure S2B, Supporting Information, shows sequence alignment of the activation loop of various STE20 protein kinases. Thr/Ser^{184} and Thr^{188} are highly conserved among various kinases of this family, and it is plausible that phosphorylation at these sites is critical for the activation of other protein kinases. On the other hand, many protein kinases in STE20 family have Ser/Thr at position 178 and phosphorylation at the site might influence the kinase activity in this family.

Autophosphorylation of the Kinase Domain Activates the Protein Kinase Activity. To see whether autophosphorylation in the kinase domain regulates the protein kinase activity of Myo3A, we examine the effect of autophosphorylation on the protein kinase activity using myelin basic protein (MBP) as a common substrate. The hMyo3A-KD was first incubated with or without cold ATP; then the phosphorylation reaction was started by adding [^{32}P]-ATP, and incorporation of ^{32}P into MBP was monitored. The protein kinase activity was markedly increased by autophosphorylation (Figure S3, Supporting Information). Note that no ^{32}P incorporation to hMyo3A-KD was detected for the prephosphorylated hMyo3A-KD, which suggests that the phosphorylation sites were saturated with phosphorylation with cold ATP during preincubation for 90 min.

Determination of the Predominant Phosphorylation Sites. In order to investigate the predominant autophosphorylation sites, we performed site-directed mutagenesis, in which the phosphorylation sites (Ser^{73}, Ser^{177}, Thr^{178}, Thr^{184}, Thr^{188}, and Thr^{302}) were substituted for Ala (S73A, S177A, T178A, T184A, T188A, and T302A). The hMyo3A-KD derivatives were measured for autophosphorylation activity in the presence of [γ-^{32}P]ATP (at 25 °C for 5 min), and subjected to phosphoimage analysis.

Phosphoimage analysis revealed that T178A, T184A, and T188A mutations decreased the autophosphorylation and MBP phosphorylation activities of hMyo3A-KD (Figure 2A). On the other hand, S73A, S177A, and T302A mutations did not notably reduce autophosphorylation. These results suggest that Ser^{73}, Ser^{177}, and Thr^{302} are not important for autophosphorylation activity of hMyo3A-KD. Consistently, T178A, T184A, and T188A mutants showed a marked decrease in the protein kinase activity against MBP (Figure 2B). These results suggest that Thr^{178}, Thr^{184}, and Thr^{188} are important for the kinase activity and autophosphorylation of hMyo3A-KD. The effect of mutation of these sites on autophosphoryation was examined in more detail.

The T178A mutant was autophosphorylated with prolonged time although the phosphorylation was significantly slower than that for the wild-type (WT) (Figure 2B). Both T184A and T188A mutants failed to be autophosphorylated even with prolonged phosphorylation time (Figure 2B). These results suggest that Thr^{184} and Thr^{188} are important for the autophosphorylation/protein kinase activity of Myo3A. These results are consistent with Figure 1C, which shows that predominant autophosphorylation sites are threonine residues.

It is possible that the purified hMyo3A-KD is phosphorylated at certain sites prior to the autophosphorylation reaction. To determine the major sites phosphorylated during the autophosphorylation reaction, we prepared hMyo3A-KD(D150N), which

dx.doi.org/10.1021/bi501247z | Biochemistry 2014, 53, 7835−7845

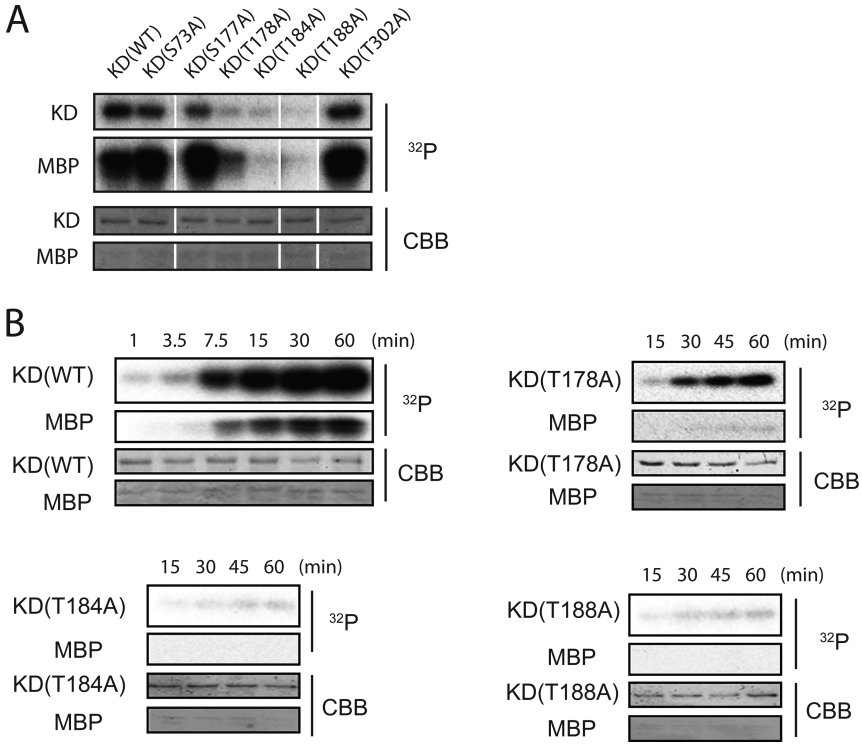

Figure 2. Effect of mutation of each phosphorylation site on protein kinase activity of hMyo3A-KD. (A) Effect of mutation at the phosphorylation sites on the protein kinase activity and autophosphorylation of hMyo3A-KD. Upper, phosphoimages; lower, input amount of hMyo3A-KD mutants and myelin basic protein (MBP) stained with Coomassie Brilliant Blue R-250. hMyo3A-KD mutants (1 μg) were incubated with 0.25 mM [γ-^{32}P]ATP and myelin basic protein (MBP) for 5 min at 25 °C. (B) Time course of autophosphorylation and MBP phosphorylation of hMyo3A-KD mutants. Upper, phosphoimages; lower, input amount of hMyo3A-KD mutants and myelin basic protein (MBP) stained with Coomassie Brilliant Blue R-250. Reaction conditions are the same as in panel A.

has no kinase activity, and examined the phosphorylation by the wild-type hMyo3A-KD (Figure 3). T184A mutation markedly decreased phosphorylation of hMyo3A-KD(D150N) by the wild-type hMyo3A-KD. On the other hand, while T188A mutation reduced wild-type hMyo3A-KD induced phosphorylation, the effect was not as much as that of T184A mutation. The result suggests that Thr^{188} of isolated hMyo3A-KD is phosphorylated to a certain extent, and Thr^{184} is the major site phopshorylated during the phosphorylation reaction.

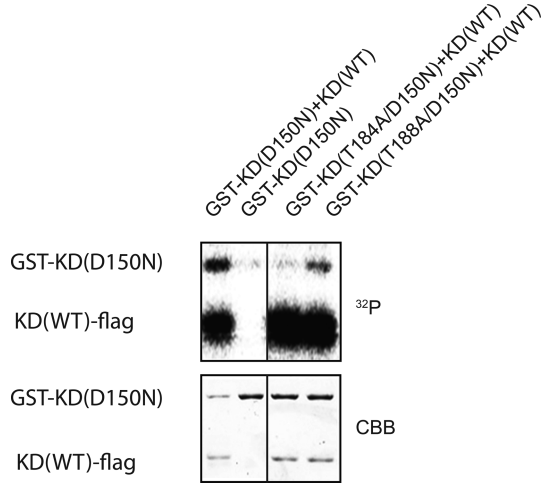

Figure 3. ^{32}P incorporation of the inactive KD catalyzed by wild type KD. GST-KD(D150N) having no intrinsic kinase activity was incubated with the wild-type KD in the presence of [γ-^{32}P]ATP and incorporation of ^{32}P was monitored by autoradiography. Upper, autoradiography; lower, Coomassie Brilliant Blue staining of the gel.

Phosphorylation of the Motor Domain of Myosin IIIA by hMyo3A-KD. It has been shown that the KD phosphorylates the motor domain of Myo3A.[12,13] We purified the motor domain without the KD (hMyo3A-MDIQo) and studied the effect of mutation of the phosphorylation sites in the KD on the phosphorylation of the motor domain.

The mutation of Thr^{184} and Thr^{188} markedly diminished the phosphorylation of hMyo3A-MDIQo (Figure 4). It was shown previously that the phosphorylation of the motor domain inhibits its actin-activated ATPase activity.[12,13] Therefore, these results suggest that the phopshorylation of Thr^{184} and Thr^{188} is important for the regulation of the motor activity of Myo3A. To address this issue, we measured the actin-activated ATPase activity of hMyo3A-MDIQo in the presence of each hMyo3A-KD derivative. hMyo3A-MDIQo was preincubated with each hMyo3A-KD derivative for 1 h in the presence of 1 mM ATP, then F-actin was added to start the actin-activated ATPase reaction. Addition of the KD(WT) significantly diminished the actin-activated ATPase activity of hMyo3A-MDIQo, which is thought to be due to phosphorylation of the motor domain.

The ATPase activities of hMyo3A-MDIQo preincubated with either hMyo3A-KD(T184A) or hMyo3A-KD(T188A) were similar to that in the absence of hMyo3A-KD (Figure 5). This result is consistent with the result that these mutations inhibit the kinase activities of the KD (Figure 2). On the other hand, KD(T178A) inhibited the ATPase activity to the same extent as KD(WT) (Figure 5). These results strongly suggest that Thr^{184}

dx.doi.org/10.1021/bi501247z | Biochemistry 2014, 53, 7835−7845

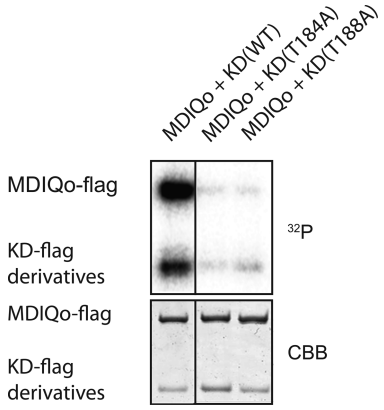

Figure 4. Phosphorylation of the motor domain of hMyo3A by hMyo3A-KD variants: (lane 1) hMyo3A-MDIQo and KD(WT); (lane 2) hMyo3A-MDIQo and KD(T184A); (lane 3) hMyo3A-MDIQo and KD(T188A). The bottom panel indicates input amount of hMyo3A-MDIQo and hMyo3A variants stained with Coomassie Brilliant Blue R-250. The reaction was done with 36 nM of hMyo3A-KD variants, 36 nM of hMyo3A-MDIQo, and 0.25 mM [γ-^{32}P] ATP at 25 °C for 1 h.

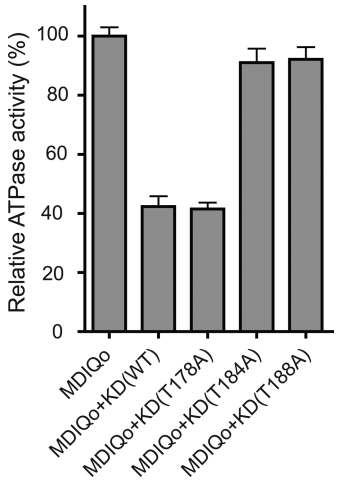

Figure 5. Effect of the mutation at the kinase domain on the actin activated ATPase activity of the motor domain of hMyo3. Actin activated ATPase activity was measured as described in Experimental Procedures. The ATPase activity of hMyo3A-MDIQo phosphorylated by each hMyo3A-KD variant is compared with hMyo3A-MDIQo without phosphorylation by hMyo3A-KD. The relative activities of hMyo3A-MDIQo with each hMyo3A-KD variant are shown. The actin-activated ATPase activity (100%) is 0.82 ± 0.05 s^{-1}. The data shown are the means of at least three independent experiments.

and Thr^{188} of the kinase domain are the most important sites for the kinase activity.

Binding of the KD to the Motor Domain. To study whether the KD has a binding activity to the motor domain, we performed motor domain pull-down assay using GST-KD derivatives. GST-KD was autophopshorylated prior to the binding assay. The phosphorylated GST-KD did pull-down the motor domain (hMyo3A-MDIQo), while GST alone failed to pull-down hMyo3A-MDIQo, suggesting that the KD has a binding activity to the motor domain (Figure S4, lanes 1 and 2, Supporting Information). We asked the question whether autophosphorylation of kinase domain influences the binding to the moror domain. To address this question, each KD mutant was subjected to the binding assay. None of the muations including T184A and T188A influenced the binding of GST-KD to hMyo3A-MDIQo (Figure S4, Supporting Information). The result suggests that the kinase domain interacts with the motor domain, which may facilitate the phosphorylation of the motor domain; however, the phosphorylation of the KD or the kinase activity of the KD does not influence the interaction between the KD and the motor domain.

The Kinase Activity Influences the Translocation of Full-length hMyo3A to the Tip of Microvilli. It has been found that Myo3A localizes at the tip of stereocilia in inner ear hair cells and the plus ends of actin filament bundles of the microvilli-like calycal processes.[2,3] Therefore, we studied the role of phosphorylation at critical sites in the KD on translocation of Myo3A in microvilli, an actin bundle structure similar to stereocilia. When Caco2 cells were transfected with espin 1, thin and short microvilli-like protrusions were produced from the apical surface of the cells (Figure 6A). Coexpression of full-length human myosin IIIA (hMyo3A(WT)) induced much longer and thicker microvilli-like apical protrusions (Figure 6B). It was previously reported that Myo3A elongates the length of filopodia induced by espin 1 in Cos7 cells,[16] and the present result is consistent with the earlier report. Moreover, our result suggests that Myo3A ties-up the actin bundles produced by espin 1 to make thick and long microvilli-like protrusive structures. Espin 1 localizes throughout the microvilli, and hMyo3A(WT) well colocalized with espin 1 throughout the microvilli but did not show discrete localization within the microvilli (Figure 6B). On the other hand, hMyo3A(D150N), a kinase dead variant of full-length myosin IIIA, showed discrete localization at the tips of microvilli (Figure 6C). This suggests that the kinase activity, and thus autophosphorylation, attenuates the microvilli tip localization of Myo3A. On the other hand, elimination of the kinase activity did not change the distribution of espin 1 in the microvilli. The result suggests that the majority of Myo3A may not efficiently transport espin 1 or transported espin 1 is immediately pushed back together with actin because of fast actin treadmill. We then asked a question of which residues in the KD are critical for the translocation of Myo3A in microvilli. To address this question, we coexpressed GFP−full length hMyo3A(T184A) and hMyo3A(T188A) with espin 1 in Caco2 cell (Figure 6D,E). GFP−full length hMyo3A(T184A) and hMyo3A(T188A) showed significant accumulation at the tip of microvilli (Figure 6D,E). It should be noted that these mutant Myo3A did not alter the localization of espin 1 in microvilli. These results suggest that autophosphorylation at Thr^{184} and Thr^{188} is critical for the translocation of Myo3A in cells. These results are consistent with the role of these sites on autophosphorylation of the KD, in which Thr^{184} and Thr^{188} are critical for autophosphorylation.

Identification of hMyo3A Specific PPase. Since the extent of phosphorylation of Myo3A is controlled by the relative rate of autophosphorylation and dephosphorylation by protein phosphatase (PPase), we attempted to identify the protein phosphatases responsible for the dephosphorylation of Myo3A. To identify hMyo3A specific PPase, we examined the dephosphorylation of hMyo3A-KD using retina tissue extracts with or without PPase inhibitors, okadaic acid (OA) and tautomycetin (TMC), which distinguish the different types of PPases (Figure 7A,B).

The hMyo3A-KD specific PPase activity was significantly inhibited by a low concentration (IC_{50} = 2 nM) of OA, whereas the inhibition required high concentration (IC_{50} = 93 nM) of TMC (Figure 7A,B). This result suggests that the hMyo3A-KD specific PPase is type 2A PPase. To confirm this, we made

dx.doi.org/10.1021/bi501247z | Biochemistry 2014, 53, 7835−7845

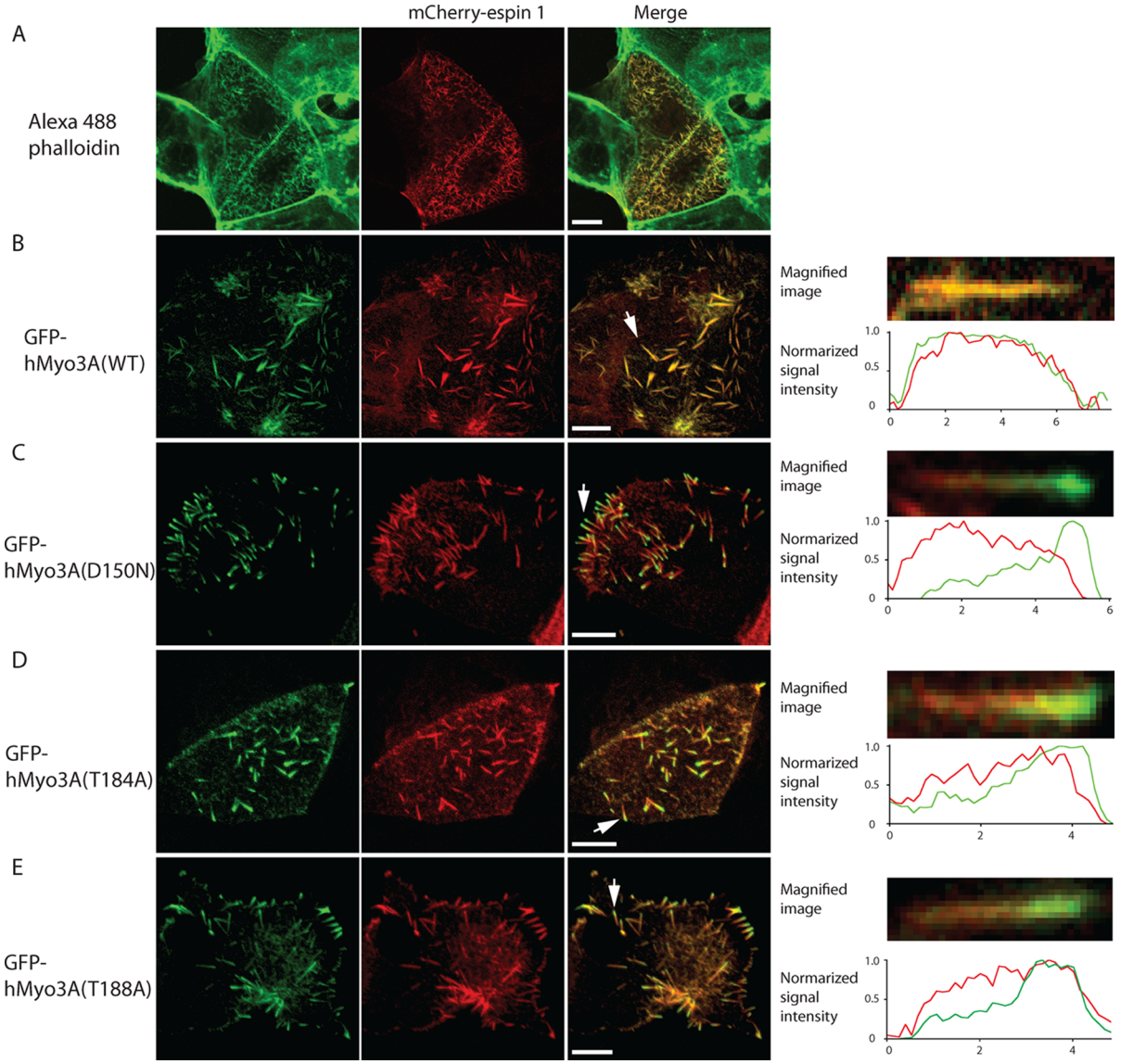

Figure 6. Effect of hMyo3A on microvilli formation and localization of espin 1 and hMyo3A in microvilli. Caco2 cells were transfected with mCherry−espin 1 (A) or cotransfected with GFP−full length hMyo3A (GFP−hMyo3A) (B), GFP−hMyo3A(D150N) (C), GFP−hMyo3A(T184A) (D), or GFP−hMyo3A (T188A) (E). (left) Alexa-568 phalloidin staining (A) or GFP−hMyo3A constructs (B−F); (middle) mCherry−espin 1; (right) merged images. Right panels show representative magnified images of microvilli. Normalized signal intensities of GFP and mCherry along the microvilli are also shown in the lower panels.

recombinant phosphatase type 1 catalytic domain (PP1c) and phosphatase type 2A catalytic domain (PP2Ac) and measured the dephosphorylation of phosphorylated hMyo3A-KD (Figure 8). The recombinant PP2Ac markedly dephosphorylated hMyo3A-KD, whereas PP1c showed low activity in dephosphorylation of hMyo3A-KD (Figure 8A), although both recombinant PPases showed similar dephosphorylation activity for LC_{20} (Figure 8B). Figure 8C−E shows the inhibition of PP2Ac for dephosphorylation of hMyo3A-KD. The concentration dependence of the inhibition by OA and TMC is nearly identical to that of Myo3A phosphatase in retina extract (see Figure 7). This result further supports that PPase type 2A is responsible for dephosphorylation of hMyo3A.

Since phosphorylation in the motor domain regulates the affinity of hMyo3A to actin, we examined dephosphorylation of the hMyo3A-MDIQo by retina extract, PP1c, and PP2Ac (Figure S5, Supporting Information). hMyo3A-MDIQo was first phosphorylated by hMyo3A-KD and then subjected to dephosphorylation in the presence of retina extract, PP1c, and PP2Ac. The hMyo3A-MDIQo was dephosphorylated by retina extract or PP2Ac, whereas PP1c did not effectively dephosphorylate the motor domain. Interestingly, both PP1c and PP2Ac showed higher dephosphorylation activity for the kinase domain than for the motor domain.

■ DISCUSSION

Six phosphorylation sites in the KD of human Myo3A are identified by mass spectrometry analysis in the present study. Four out of six identified phosphorylation sites in KD were located at the activation loop (Ser^{177}, Thr^{178}, Thr^{184}, and Thr^{188}). All four residues are conserved among myosin IIIs from various species, and all but Ser^{177} are also conserved among Msn kinases belonging to the STE20 kinase family. The result suggests that these protein kinases are also autophosphorylated at these residues, which regulate the kinase activity.

dx.doi.org/10.1021/bi501247z | *Biochemistry* 2014, 53, 7835−7845

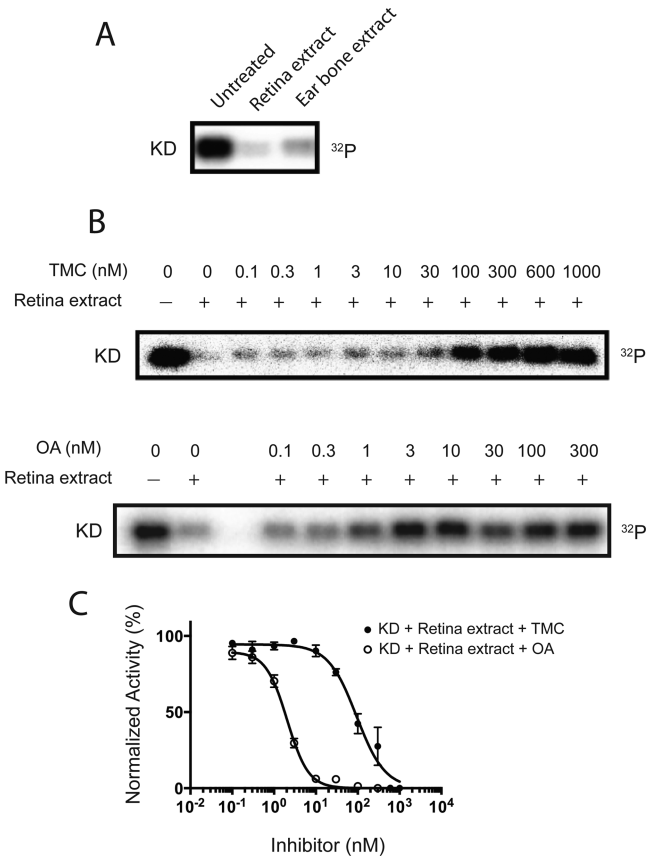

Figure 7. Identification of hMyo3A-KD specific PPase from pig retina. (A) Phosphorylated hMyo3A-KD (P-KD, 36 nM) was incubated with tissue extracts (pig retina and ear bone) for 30 min. (lane 1) P-KD alone; (lane 2) P-KD and 50 μg/mL of retina tissue extract; (lane 3) P-KD and 50 μg/mL of ear bone extract. (B) (upper) Dephosphorylation of 36 nM of P-KD by retina extract (50 μg/mL) with various TMC concentration: (lane 1) P-KD alone; (lane 2) P-KD and 50 μg/mL of retina tissue extract; (lanes 3−12) P-KD and 10 μg/mL retina tissue extract with various TMC concentrations as indicated. (lower) Dephosphorylation of 36 nM of P-KD by retina tissue extract (50 μg/mL) with various OA concentration: (lane 1) P-KD alone; (lane 2) P-KD with retina tissue extract; (lanes 3−7) P-KD and 10 μg/mL retina tissue extract with various OA concentrations as indicated. (C) PPase activity determined by measuring the decrease in the radioactivity in panel B. The data shown in the graph represent mean ± SEM from three independent sets of experiments. The radioactive band was excised and subjected to Cerenkov counting. The value of untreated was set as 100%. IC_{50} of OA and TMA was 2 nM and 93 nM, respectively.

Two phosphorylation sites, Ser^{177} and Thr^{184} in mouse Myo3A, were previously reported.[30] While this study was underway, Ser^{177}, Thr^{178}, and Thr^{184} were reported as phosphorylation sites in the KD of hMyo3A.[18] These sites are also identified in hMyo3A in this study. Thr^{184} of hMyo3A site was identified as a major autophosphorylation site, but Ser^{177} and Thr^{178} were not major sites, and S177A and T178A mutation did not affect the autophosphorylation of the KD. Furthermore, we newly identified an additional predominant site (Thr^{188}) in hMyo3A-KD, which is located in the activation loop of the kinase domain. Among these sites, T184A and T188A mutation notably diminished the kinase activity, suggesting that the phosphorylation of these sites activates the kinase. T184A and T188A mutation almost completely inhibited the autophosphorylation activity.

It is known that phosphorylation in the activation loop activates various protein kinases.[31] For instance, PKA[32] and PKC[33] are phosphorylated at Thr^{197} and Thr^{500} [PKC βII[34]], respectively, corresponding to Thr^{184} of hMyo3A, in the activation loop catalyzed by PDK1,[35] which causes marked activation of the kinase activity. Our result suggests that Thr^{184} is one of the major sites of autophosphorylation, and the phosphorylation at this site notably enhances the kinase activity. While other protein kinases such as PDK1 might also phosphorylate this site for activation, based upon our present result, it is likely that Myo3A is autophosphorylated in cells. Threonine at this site is replaced by other residues in several STE20 families (Figure S2B, Supporting Information).

We also found that Thr^{188} is phosphorylated and T188A mutation markedly diminishes the kinase activity. This residue is pretty well conserved among Ser/Thr kinases with some exceptions, but this residue is replaced by proline for tyrosine kinases.[36] In some kinases in STE20 family, the threonine residue at this position is replaced by valine or cysteine (Figure S2B, Supporting Information).

When this site of the inactive KD is mutated to alanine, notable ^{32}P incorporation is achieved by active KD, which suggests that a significant fraction of Thr^{188} is phosphorylated before the ^{32}P incorporation reaction. Alternatively, prior phosphorylation of Thr^{184} is required for the phosphorylation of Thr^{188}.

Taken together, it is thought that the phosphorylation of Thr^{188} is critical for the activation of the kinase activity and the phosphorylation at this site may not be readily dephosphorylated by protein phosphatases. It was reported previously for PKA that T201A mutation (corresponding to Thr^{188} of hMyo3A) reduced the protein kinase activity. It was suggested that the −OH moiety of Thr^{201} is within hydrogen bonding distance from Lys^{168}, which has an important role in the transfer of γ-phosphate of ATP.[37] Since several Ser/Thr kinases have valine and cysteine, and tyrosine kinases have proline in this position, it is not clear whether the threonine residue at this position hydrogen bonds with lysine in the catalytic lobe. However, we cannot exclude a possibility that T188A mutation inactivates the activity due to disruption of hydrogen bonding.

On the other hand, incorporation of ^{32}P was markedly reduced for T184A mutation, suggesting that the Thr^{184} site is easily available for autophosphorylation and is susceptible to dephosphorylation reaction. Since Myo3A autophosphorylates this site, it is plausible that this site is phosphorylated in cells in basal conditions and the dephosphorylation can be achieved upon the activation of the responsible protein phosphatases.

An important question is the identity of such protein phosphatases. Present results demonstrated that protein phosphatase type 2A is responsible for the dephopshorylation of Myo3A for both the kinase domain and the motor domain. When Caco2 cells were transfected with the wild-type Myo3A, it did not localize at the tip of microvilli. This suggests that Myo3A is in the phosphorylated form, since the unphosphorylatable constructs showed the tip localization (Figure 6). It is plausible that PP2A needs to be activated for translocation of hMyo3A to the tip of microvilli.

Previous studies showed that full length Myo3A and espin 1 colocalize at filopodia in Cos7 cells without discrete localization.[16] However, the elimination of the kinase domain of Myo3A induced accumulation of espin 1 and full length Myo3A at filopodial tips.[16] Since phosphorylation of the motor domain of Myo3A markedly changes the affinity for actin,[12,13] it is thought that dephosphorylation of Myo3A facilitates the

dx.doi.org/10.1021/bi501247z | Biochemistry 2014, 53, 7835−7845

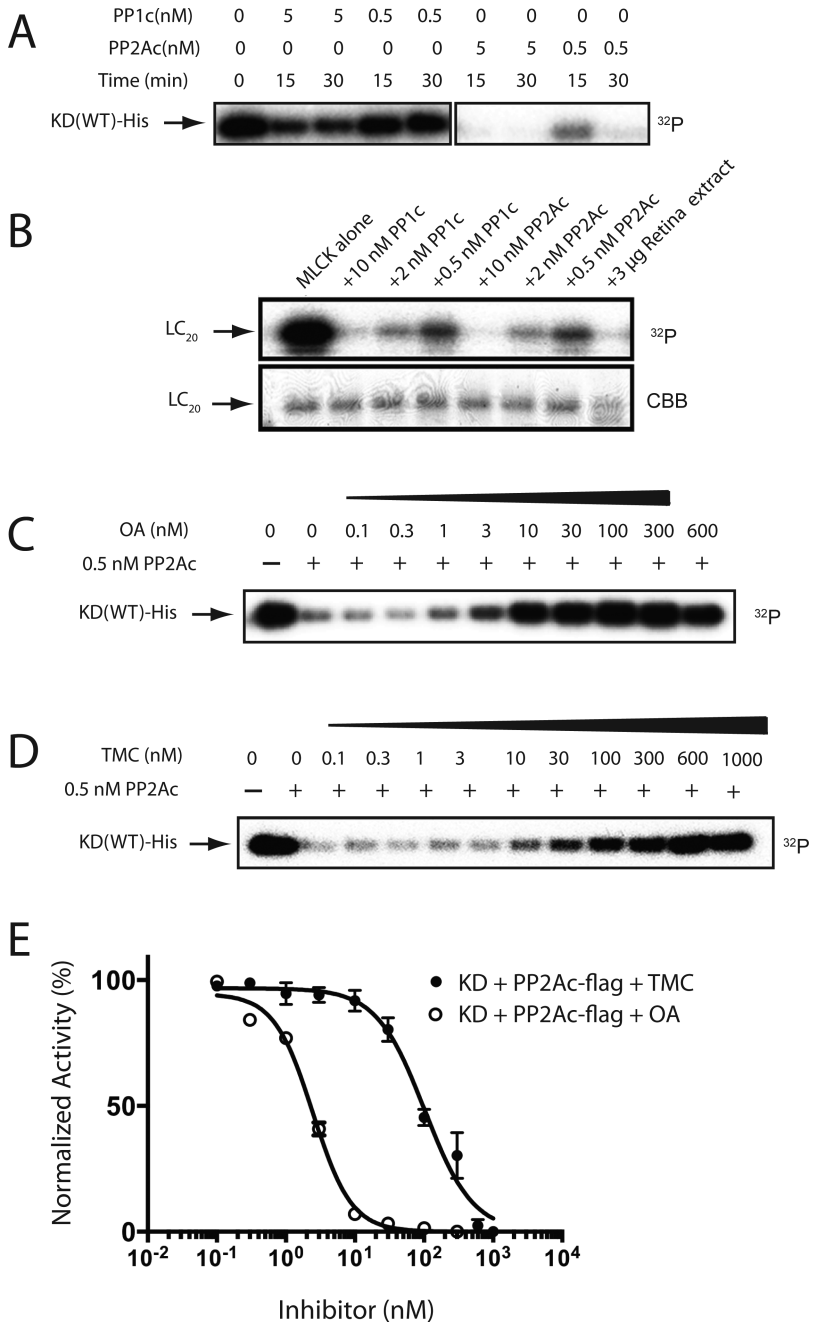

Figure 8. Dephosphorylation of hMyo3A-KD by isolated PPases. (A) Dephopshorylatipon of hMyo3A-KD by PP1c and PP2Ac. Decrease of ^{32}P in 36 nM of phosphorylated-KD was monitored by autoradiography: (lane 1) P-KD alone; (lanes 2 and 3) P-KD with 5 nM of PP1c for 15 and 30 min, respectively; (lanes 4 and 5) P-KD with 0.5 nM of PP1c for 15 and 30 min, respectively; (lanes 6 and 7) P-KD with 5 nM of PP2Ac for 15 and 30 min, respectively; (lanes 8 and 9) P-KD with 0.5 nM of PP2Ac for 15 and 30 min, respectively. (B) Dephosphorylation of LC_{20} by PP1c and PP2Ac. Decrease of [^{32}P] in 50 μg/mL of P-LC_{20} was monitored: (lane 1) P-LC_{20} alone; (lane 2) P-LC_{20} with 10 nM PP1c; (lane 3) P-LC_{20} with 2 nM PP1c, (lane 4) P-LC_{20} with 0.5 nM of PP1c; (lane 5) P-LC_{20} with 10 nM of PP2Ac; (lane 6) P-LC_{20} with 2 nM PP2Ac; (lane 7) P-LC_{20} with 0.5 nM PP2Ac; (lane 8) P-LC_{20} with 50 μg/mL of retina tissue extract. The reaction time was 30 min. The bottom panel indicates input stained with Coomassie Brilliant Blue R-250. (C) Inhibition of PP2Ac dependent dephosphorylation of hMyo3A-KD by various concentrations of OA: (lane 1) P-KD alone; (lanes 2−10) P-KD and 0.5 nM of PP2Ac in the presence of the indicated amount of OA. (D) Inhibition of PP2Ac dependent dephosphorylation of hMyo3A-KD by various concentration of TMC: (lane 1) P-KD alone; (lanes 2−12) P-KD dephosphorylated by 0.5 nM of PP2Ac with various TMC concentration indicated. (E) Inhibition of PP2Ac as a function of OA and TMC concentration. The graph represents mean ± SEM from three independent sets of experiments. The radioactive band was excised and subjected to Cerenkov counting. The value without PP2Ac was set as 100%.

translocation of Myo3A due to the increase in the affinity for actin, and it transports espin 1 to filopodial tips. However, Myo3A and espin 1 are found in stereocilia, a microvilli-like structure, in vivo.[16] Moreover, it was found that single nucleotide polymorphisms of the *Myo3A* gene are linked with an increase in risk for colon cancer.[38] Therefore, we used microvilli of a colon cancer cell line (Caco2) as a model to investigate the function of Myo3A in vivo.

We found that espin 1 induced thin and short protrusions in Caco2 cells. The result is consistent with the finding in a kidney

dx.doi.org/10.1021/bi501247z | *Biochemistry* 2014, 53, 7835−7845

epithelial cell line, LLC-PK1-CL4, in which overexpression of espin 1 induced actin bundles to form apical protrusions.[39] Interestingly, we found that coexpression of Myo3A with espin 1 induced much thicker and longer microvilli-like apical protrusions, and Myo3A and espin 1 colocalized throughout the body of microvilli. This result is consistent with the finding that Myo3A binds to espin 1.[16] Furthermore, our result suggests that Myo3A influences the function of espin 1 to facilitate actin bundles. In contrast to the observation of Myo3A/espin 1 in filopodia, Myo3A does not alter the localization of espin 1 in microvilli, and espin 1 localized throughout the microvilli, although the kinase dead Myo3A was localized at the tip of microvilli. These results suggest that Myo3A does not transport espin 1, although it can bind to espin 1. It was shown previously that the Myo3A binding domain (ankyrin repeats domain) of espin 1 without the actin binding site translocates to filopodial tips along with Myo3A.[16] Together with the present results, it is thought that espin 1 can move together with Myo3A if the actin binding activity is eliminated, but espin 1 having the actin binding activity associates with large actin bundles in microvilli. It is plausible that espin 1 ends up showing colocalization with Myo3A due to its binding affinity to Myo3A. The present finding supports this notion, and it is likely that the distribution of espin 1 is dependent on the affinity with actin and Myo3A. Based upon these findings, we propose the following model: Myo3A and espin 1 form a complex composed of multiple Myo3A/espin 1 molecules. This complex binds to a number of actin filaments to produce large actin bundles, thus creating a thick microvilli structure.

Myo3A is recruited to the espin 1 induced original apical thin protrusion through the binding to espin 1 presumably by diffusion, and once it forms a complex with espin 1, it facilitates production of large actin bundles because the complex containing multiple espin 1 molecules can converge multiple actin filaments.

We also found that the length of microvilli is notably increased with Myo3A coexpression. It is postulated that tight actin bundles containing a large number of actin filaments at the tip of the protrusion increases the density of plus ends of actin filaments. It is anticipated that this changes the equilibrium of polymerization and depolymerization of actin at the plus end toward polymerization, thus elongating microvilli, although we cannot exclude a possible function of other factors in elongation process of microvilli.

■ ASSOCIATED CONTENT

Supporting Information

Amino acid sequence alignment of myosin III and comparison of myosin III with Msn protein kinases or with different species and various protein kinases, effect of autophosphorylation of hMyo3A-KD on its protein kinase activity, binding between the kinase domain and the motor domain of hMyo3A, and dephopshorylation of the motor domain of human myosin IIIA by PPases. This material is available free of charge via the Internet at http://pubs.acs.org.

■ AUTHOR INFORMATION

Corresponding Author

*Mitsuo Ikebe. Tel: (903) 877-7785. Fax: (903) 877-5438. E-mail: Mitsuo.Ikebe@uthct.edu.

Author Contributions

B.A. and T.S. contributed equally to this work. B.A., T.S., S.K., and M.I. conceived the experiments, designed the experiments, and wrote the manuscript. H.K., S.K., and J.E. performed LC-MS/MS experiments and data analysis. R.I. performed molecular cloning and produced the expression vectors.

Funding

This study was supported by NIH Grants AR048526, DC006103, and AR048898 and Korea Basic Science Institute Grant.

Notes

The authors declare no competing financial interest.

■ ABBREVIATIONS:

hMyo3A, Human myosin IIIA; KD, kinase domain; OA, okadaic acid; TMC, tautomycetin; MBP, myelin basic protein; RLC, regulatory light chain; PPase, protein phosphatase; MSN, Ste20-related kinase, misshapen; PP2A, protein phosphatase type 2A

■ REFERENCES

(1) Montell, C., and Rubin, G. M. (1988) The *Drosophila* ninaC locus encodes two photoreceptor cell specific proteins with domains homologous to protein kinases and the myosin heavy chain head. *Cell 52*, 757−772.

(2) Dose, A. C., Hillman, D. W., Wong, C., Sohlberg, L., Lin-Jones, J., and Burnside, B. (2003) Myo3A, one of two class III myosin genes expressed in vertebrate retina, is localized to the calycal processes of rod and cone photoreceptors and is expressed in the sacculus. *Mol. Biol. Cell 14*, 1058−1073.

(3) Schneider, M. E., Dose, A. C., Salles, F. T., Chang, W., Erickson, F. L., Burnside, B., and Kachar, B. (2006) A new compartment at stereocilia tips defined by spatial and temporal patterns of myosin IIIa expression. *J. Neurosci. 26*, 10243−10252.

(4) Dose, A. C., and Burnside, B. (2000) Cloning and chromosomal localization of a human class III myosin. *Genomics 67*, 333−342.

(5) Dose, A. C., and Burnside, B. (2002) A class III myosin expressed in the retina is a potential candidate for Bardet-Biedl syndrome. *Genomics 79*, 621−624.

(6) Walsh, T., Walsh, V., Vreugde, S., Hertzano, R., Shahin, H., Haika, S., Lee, M. K., Kanaan, M., King, M. C., and Avraham, K. B. (2002) From flies' eyes to our ears: Mutations in a human class III myosin cause progressive nonsyndromic hearing loss DFNB30. *Proc. Natl. Acad. Sci. U. S. A. 99*, 7518−7523.

(7) Walsh, V. L., Raviv, D., Dror, A. A., Shahin, H., Walsh, T., Kanaan, M. N., Avraham, K. B., and King, M. C. (2011) A mouse model for human hearing loss DFNB30 due to loss of function of myosin IIIA. *Mamm. Genome 22*, 170−177.

(8) Hardie, R. (2002) Adaptation through translocation. *Neuron 34*, 3−5.

(9) Hardie, R. C. (2003) Phototransduction: Shedding light on translocation. *Curr. Biol. 13*, R775−777.

(10) Sokolov, M., Lyubarsky, A. L., Strissel, K. J., Savchenko, A. B., Govardovskii, V. I., Pugh, E. N., Jr., and Arshavsky, V. Y. (2002) Massive light-driven translocation of transducin between the two major compartments of rod cells: A novel mechanism of light adaptation. *Neuron 34*, 95−106.

(11) Les Erickson, F., Corsa, A. C., Dose, A. C., and Burnside, B. (2003) Localization of a class III myosin to filopodia tips in transfected HeLa cells requires an actin-binding site in its tail domain. *Mol. Biol. Cell 14*, 4173−4180.

(12) Kambara, T., Komaba, S., and Ikebe, M. (2006) Human myosin III is a motor having an extremely high affinity for actin. *J. Biol. Chem. 281*, 37291−37301.

(13) Komaba, S., Watanabe, S., Umeki, N., Sato, O., and Ikebe, M. (2010) Effect of phosphorylation in the motor domain of human myosin IIIA on its ATP hydrolysis cycle. *Biochemistry 49*, 3695−3702.

(14) Komaba, S., Inoue, A., Maruta, S., Hosoya, H., and Ikebe, M. (2003) Determination of human myosin III as a motor protein having a protein kinase activity. *J. Biol. Chem. 278*, 21352−21360.
(15) Dose, A. C., Ananthanarayanan, S., Moore, J. E., Burnside, B., and Yengo, C. M. (2007) Kinetic mechanism of human myosin IIIA. *J. Biol. Chem. 282*, 216−231.
(16) Salles, F. T., Merritt, R. C., Jr., Manor, U., Dougherty, G. W., Sousa, A. D., Moore, J. E., Yengo, C. M., Dose, A. C., and Kachar, B. (2009) Myosin IIIa boosts elongation of stereocilia by transporting espin 1 to the plus ends of actin filaments. *Nat. Cell Biol. 11*, 443−450.
(17) Quintero, O. A., Moore, J. E., Unrath, W. C., Manor, U., Salles, F. T., Grati, M., Kachar, B., and Yengo, C. M. (2010) Intermolecular autophosphorylation regulates myosin IIIa activity and localization in parallel actin bundles. *J. Biol. Chem. 285*, 35770−35782.
(18) Quintero, O. A., Unrath, W. C., Stevens, S. M., Jr., Manor, U., Kachar, B., and Yengo, C. M. (2013) Myosin 3A kinase activity is regulated by phosphorylation of the kinase domain activation loop. *J. Biol. Chem. 288*, 37126−37137.
(19) Spudich, J. A., and Watt, S. (1971) The regulation of rabbit skeletal muscle contraction. I. Biochemical studies of the interaction of the tropomyosin-troponin complex with actin and the proteolytic fragments of myosin. *J. Biol. Chem. 246*, 4866−4871.
(20) Ikebe, M., Reardon, S., Schwonek, J. P., Sanders, C. R., 2nd, and Ikebe, R. (1994) Structural requirement of the regulatory light chain of smooth muscle myosin as a substrate for myosin light chain kinase. *J. Biol. Chem. 269*, 28165−28172.
(21) Ikebe, M., Kambara, T., Stafford, W. F., Sata, M., Katayama, E., and Ikebe, R. (1998) A hinge at the central helix of the regulatory light chain of myosin is critical for phosphorylation-dependent regulation of smooth muscle myosin motor activity. *J. Biol. Chem. 273*, 17702−17707.
(22) Ikebe, M., and Hartshorne, D. J. (1985) Effects of Ca2+ on the conformation and enzymatic activity of smooth muscle myosin. *J. Biol. Chem. 260*, 13146−13153.
(23) Weiner, M. P., Costa, G. L., Schoettlin, W., Cline, J., Mathur, E., and Bauer, J. C. (1994) Site-directed mutagenesis of double-stranded DNA by the polymerase chain reaction. *Gene 151*, 119−123.
(24) Wang, F., Harvey, E. V., Conti, M. A., Wei, D., and Sellers, J. R. (2000) A conserved negatively charged amino acid modulates function in human nonmuscle myosin IIA. *Biochemistry 39*, 5555−5560.
(25) Kempler, K., Toth, J., Yamashita, R., Mapel, G., Robinson, K., Cardasis, H., Stevens, S., Sellers, J. R., and Battelle, B. A. (2007) Loop 2 of limulus myosin III is phosphorylated by protein kinase A and autophosphorylation. *Biochemistry 46*, 4280−4293.
(26) Khromykh, A. A., Harvey, T. J., Abedinia, M., and Westaway, E. G. (1996) Expression and purification of the seven nonstructural proteins of the flavivirus Kunjin in the *E. coli* and the baculovirus expression systems. *J. Virol. Methods 61*, 47−58.
(27) Laemmli, U. K. (1970) Cleavage of structural proteins during the assembly of the head of bacteriophage T4. *Nature 227*, 680−685.
(28) Shevchenko, A., Tomas, H., Havlis, J., Olsen, J. V., and Mann, M. (2006) In-gel digestion for mass spectrometric characterization of proteins and proteomes. *Nat. Protoc. 1*, 2856−2860.
(29) Reynard, A. M., Hass, L. F., Jacobsen, D. D., and Boyer, P. D. (1961) The correlation of reaction kinetics and substrate binding with the mechanism of pyruvate kinase. *J. Biol. Chem. 236*, 2277−2283.
(30) Dalal, J. S., Stevens, S. M., Jr., Alvarez, S., Munoz, N., Kempler, K. E., Dose, A. C., Burnside, B., and Battelle, B. A. (2011) Mouse class III myosins: kinase activity and phosphorylation sites. *J. Neurochem. 119*, 772−784.
(31) Adams, J. A. (2003) Activation loop phosphorylation and catalysis in protein kinases: Is there functional evidence for the autoinhibitor model? *Biochemistry 42*, 601−607.
(32) Steinberg, R. A., Cauthron, R. D., Symcox, M. M., and Shuntoh, H. (1993) Autoactivation of catalytic (C alpha) subunit of cyclic AMP-dependent protein kinase by phosphorylation of threonine 197. *Mol. Cell. Biol. 13*, 2332−2341.
(33) Cazaubon, S., Bornancin, F., and Parker, P. J. (1994) Threonine-497 is a critical site for permissive activation of protein kinase C alpha. *Biochem. J. 301* (Pt 2), 443−448.
(34) Tsutakawa, S. E., Medzihradszky, K. F., Flint, A. J., Burlingame, A. L., and Koshland, D. E., Jr. (1995) Determination of in vivo phosphorylation sites in protein kinase C. *J. Biol. Chem. 270*, 26807−26812.
(35) Chou, M. M., Hou, W., Johnson, J., Graham, L. K., Lee, M. H., Chen, C. S., Newton, A. C., Schaffhausen, B. S., and Toker, A. (1998) Regulation of protein kinase C zeta by PI 3-kinase and PDK-1. *Curr. Biol. 8*, 1069−1077.
(36) Hanks, S. K., Quinn, A. M., and Hunter, T. (1988) The protein kinase family: Conserved features and deduced phylogeny of the catalytic domains. *Science 241*, 42−52.
(37) Moore, M. J., Kanter, J. R., Jones, K. C., and Taylor, S. S. (2002) Phosphorylation of the catalytic subunit of protein kinase A. Autophosphorylation versus phosphorylation by phosphoinositide-dependent kinase-1. *J. Biol. Chem. 277*, 47878−47884.
(38) Lascorz, J., Forsti, A., Chen, B., Buch, S., Steinke, V., Rahner, N., Holinski-Feder, E., Morak, M., Schackert, H. K., Gorgens, H., Schulmann, K., Goecke, T., Kloor, M., Engel, C., Buttner, R., Kunkel, N., Weires, M., Hoffmeister, M., Pardini, B., Naccarati, A., Vodickova, L., Novotny, J., Schreiber, S., Krawczak, M., Broring, C. D., Volzke, H., Schafmayer, C., Vodicka, P., Chang-Claude, J., Brenner, H., Burwinkel, B., Propping, P., Hampe, J., and Hemminki, K. (2010) Genome-wide association study for colorectal cancer identifies risk polymorphisms in German familial cases and implicates MAPK signalling pathways in disease susceptibility. *Carcinogenesis 31*, 1612−1619.
(39) Sekerkova, G., Zheng, L., Loomis, P. A., Changyaleket, B., Whitlon, D. S., Mugnaini, E., and Bartles, J. R. (2004) Espins are multifunctional actin cytoskeletal regulatory proteins in the microvilli of chemosensory and mechanosensory cells. *J. Neurosci. 24*, 5445−5456.